© 2014. Published by The Company of Biologists Ltd | Journal of Cell Science (2014) 127, 3893–3901 doi:10.1242/jcs.135947

SHORT REPORT

CLIC3 controls recycling of late endosomal MT1-MMP and dictates invasion and metastasis in breast cancer

Iain R. Macpherson[1,2,*], Elena Rainero[1], Louise E. Mitchell[1], Peter V. E. van den Berghe[1], Claire Speirs[1], Marta A. Dozynkiewicz[1], Suman Chaudhary[1], Gabriela Kalna[1], Joanne Edwards[2], Paul Timpson[1] and Jim C. Norman[1,*]

ABSTRACT

Chloride intracellular channel 3 (CLIC3) drives invasiveness of pancreatic and ovarian cancer by acting in concert with Rab25 to regulate the recycling of α5β1 integrin from late endosomes to the plasma membrane. Here, we show that in two estrogen receptor (ER)-negative breast cancer cell lines, CLIC3 has little influence on integrin recycling, but controls trafficking of the pro-invasive matrix metalloproteinase MT1-MMP (also known as MMP14). In MDA-MB-231 cells, MT1-MMP and CLIC3 are localized primarily to late endosomal/lysosomal compartments located above the plane of adhesion and near the nucleus. MT1-MMP is transferred from these late endosomes to sites of cell–matrix adhesion in a CLIC3-dependent fashion. Correspondingly, CLIC3-knockdown opposes MT1-MMP-dependent invasive processes. These include the disruption of the basement membrane as acini formed from MCF10DCIS.com cells acquire invasive characteristics in 3D culture, and the invasion of MDA-MB-231 cells into Matrigel or organotypic plugs of type I collagen. Consistent with this, expression of CLIC3 predicts poor prognosis in ER-negative breast cancer. The identification of MT1-MMP as a cargo of a CLIC3-regulated pathway that drives invasion highlights the importance of late endosomal sorting and trafficking in breast cancer.

KEY WORDS: CLIC3, DCIS, Invasion, MT1-MMP, MMP14, Breast cancer, ER-negative, Recycling, Late endosome

INTRODUCTION

Invasion through the basement membrane and surrounding stroma is necessary for breast cancer to progress beyond the ductal carcinoma *in situ* (DCIS) stage. Matrix metalloproteinases, in particular MT1-MMP (also known as MMP14), are required for carcinoma cells to migrate across basement membranes (Hotary et al., 2006), through fibrillar type I collagen (Li et al., 2008; Sabeh et al., 2004), and for invasion and metastasis *in vivo* (Perentes et al., 2011; Sabeh et al., 2004; Szabova et al., 2008). Consistently, MT1-MMP is upregulated with increasing grade and stage of breast cancer (Ueno et al., 1997), and its expression is associated with poorer survival (McGowan and Duffy, 2008; Têtu et al., 2006). It is increasingly apparent that endocytosis and recycling of MT1-MMP provide an important level of regulation (Frittoli et al., 2011; Poincloux et al., 2009; Uekita et al., 2001; Williams and Coppolino, 2011).

We have recently shown how CLIC3 and Rab25 can cooperate to drive endocytic trafficking of active β1 integrin from the late endosome/lysosome to the plasma membrane at the rear of the cell, promoting disassembly of cell–matrix adhesion and facilitating migration (Dozynkiewicz et al., 2012). We highlighted the reduced survival following resection of operable pancreatic cancers where levels of CLIC3 were high and showed that the poorest outcomes occurred when both Rab25 and CLIC3 were elevated. Here, we report that CLIC3-dependent recycling can operate independently of Rab25 to facilitate the polarized delivery of MT1-MMP to the substratum in ER-negative MDA-MB-231 cells and show that expression of CLIC3 is associated with reduced survival in ER-negative breast cancer.

RESULTS AND DISCUSSION

CLIC3 expression is increased in breast cancer and is associated with poor outcome

To determine CLIC3 expression in breast cancer, we analyzed a tissue microarray containing primary breast carcinomas and paired adjacent normal tissue. CLIC3 staining was typically low in normal ductal epithelium with significantly higher expression in matched tumor tissue (Fig. 1A,B; supplementary material Fig. S1A,B). Consistently, the Oncomine database (Rhodes et al., 2004) identified higher levels of CLIC3 mRNA in invasive carcinomas than normal breast tissue in both the TCGA (fold increase=2.12, $P=3.18\times10^{-18}$) and Gluck (fold increase=1.60, $P=1.83\times10^{-5}$) (Glück et al., 2012) datasets (supplementary material Fig. S1C,D). Next, we investigated the relationship between CLIC3 and survival in a cohort of 141 women with ER-negative early breast cancer (Fig. 1C; supplementary material Table S1). High CLIC3 expression was associated with poorer breast-cancer-specific survival ($P=0.026$, log rank test) (Fig. 1C). Although CLIC3 expression was higher in patients with HER2-positive disease the effect of CLIC3 on survival was most evident in the HER2-negative ('triple-negative') subset (supplementary material Fig. S1E). To address whether the negative prognostic significance of CLIC3 expression could be observed in other cohorts, we analyzed gene expression data from 198 systemically untreated patients (Desmedt et al., 2007). High CLIC3 mRNA was associated with worse overall survival in the overall cohort ($P=0.039$, log rank test) (Fig. 1D) and in the subset of ER-negative ($n=64$; $P=0.005$, log rank test) (Fig. 1E), but not ER-positive (Fig. 1F) patients. These data show that CLIC3 is overexpressed in some primary breast cancers and that high levels of CLIC3 are associated with a greater risk of death.

[1]Beatson Institute for Cancer Research: Garscube Estate, Glasgow G61 1BD, UK. [2]Wolfson Wohl Cancer Research Centre, Institute of Cancer Sciences, University of Glasgow, Glasgow G61 1QH, UK.

*Authors for correspondence (iain.macpherson@glasgow.ac.uk; j.norman@beatson.gla.ac.uk)

Received 29 May 2014; Accepted 7 July 2014

Journal of Cell Science (2014) 127, 3893–3901 doi:10.1242/jcs.135947

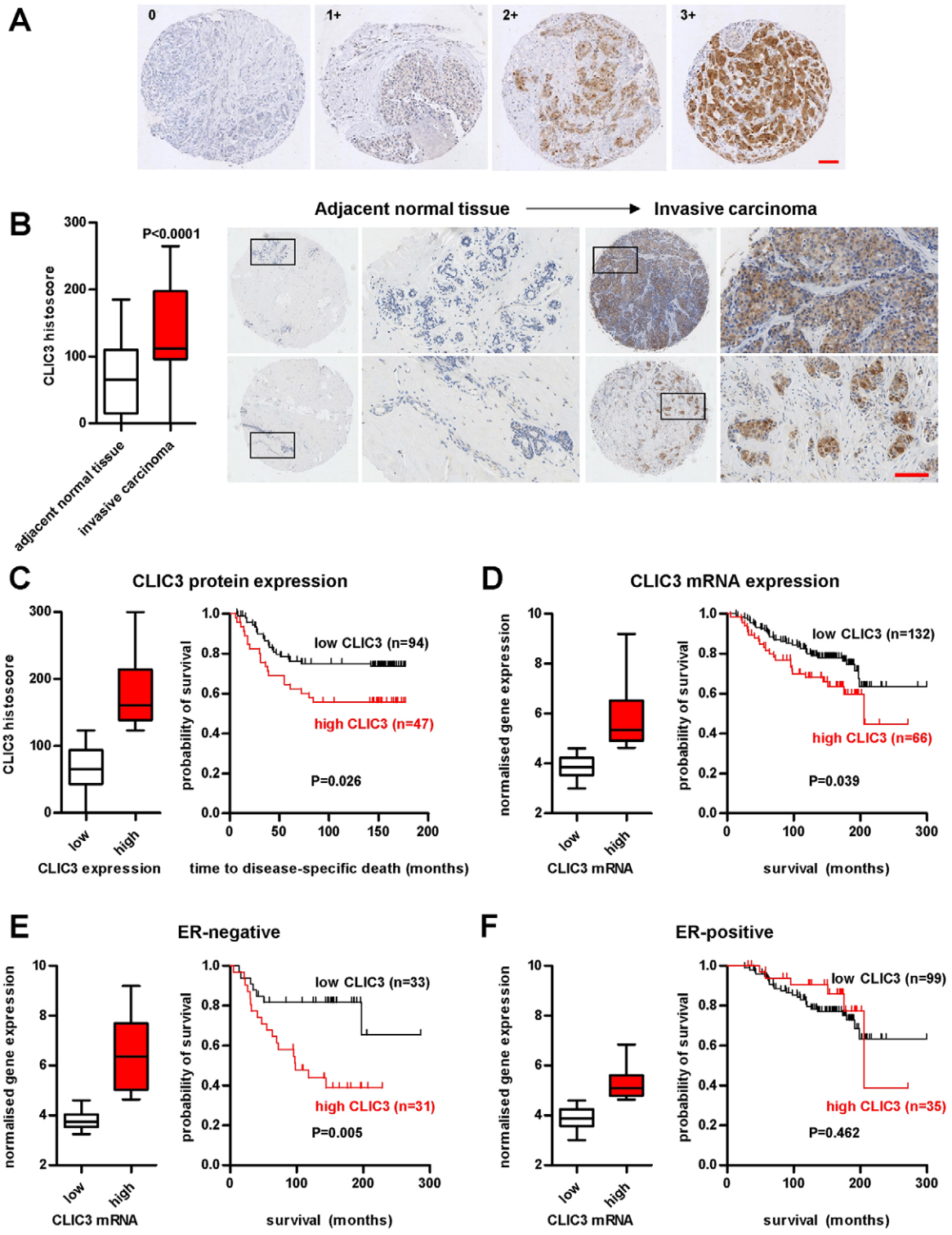

Fig. 1. CLIC3 expression is associated with poor prognosis in early breast cancer. (A) Immunohistochemical staining of CLIC3 in a breast cancer TMA indicating predominantly negative (0), weak (1+), moderate (2+) and strong (3+) staining. (B) Box plot indicating CLIC3 histoscores in invasive carcinoma and paired adjacent normal breast tissue (n=40). P-values were calculated with a Wilcoxon signed rank test. Examples of two cases with upregulated CLIC3 are shown in the right-hand TMA images. (C) Box plot illustrating stratification of patients with early breast cancer into high and low CLIC3 expressors based on histoscore (highest tertile versus lower two tertiles; H-score >123). Kaplan–Meier analysis indicates that patients with high CLIC3 protein expression have poorer breast-cancer-specific survival. (D) Kaplan–Meier analysis performed in a cohort of 198 patients with resected early breast cancer (Desmedt; GSE7390) indicating poorer overall survival in patients with high CLIC3 expression (highest tertile versus lower two tertiles). P-values were calculated with a log rank test. (E,F) Kaplan–Meier analysis of Desmedt data in subsets of patients with ER-negative (n=64; E) and ER-positive (n=134; F) disease. Scale bars: 100 μm. For box plots, the box represents the interquartile range and the middle line represents the median; whiskers represent minimum to maximum values.

Journal of Cell Science

Journal of Cell Science (2014) 127, 3893–3901 doi:10.1242/jcs.135947

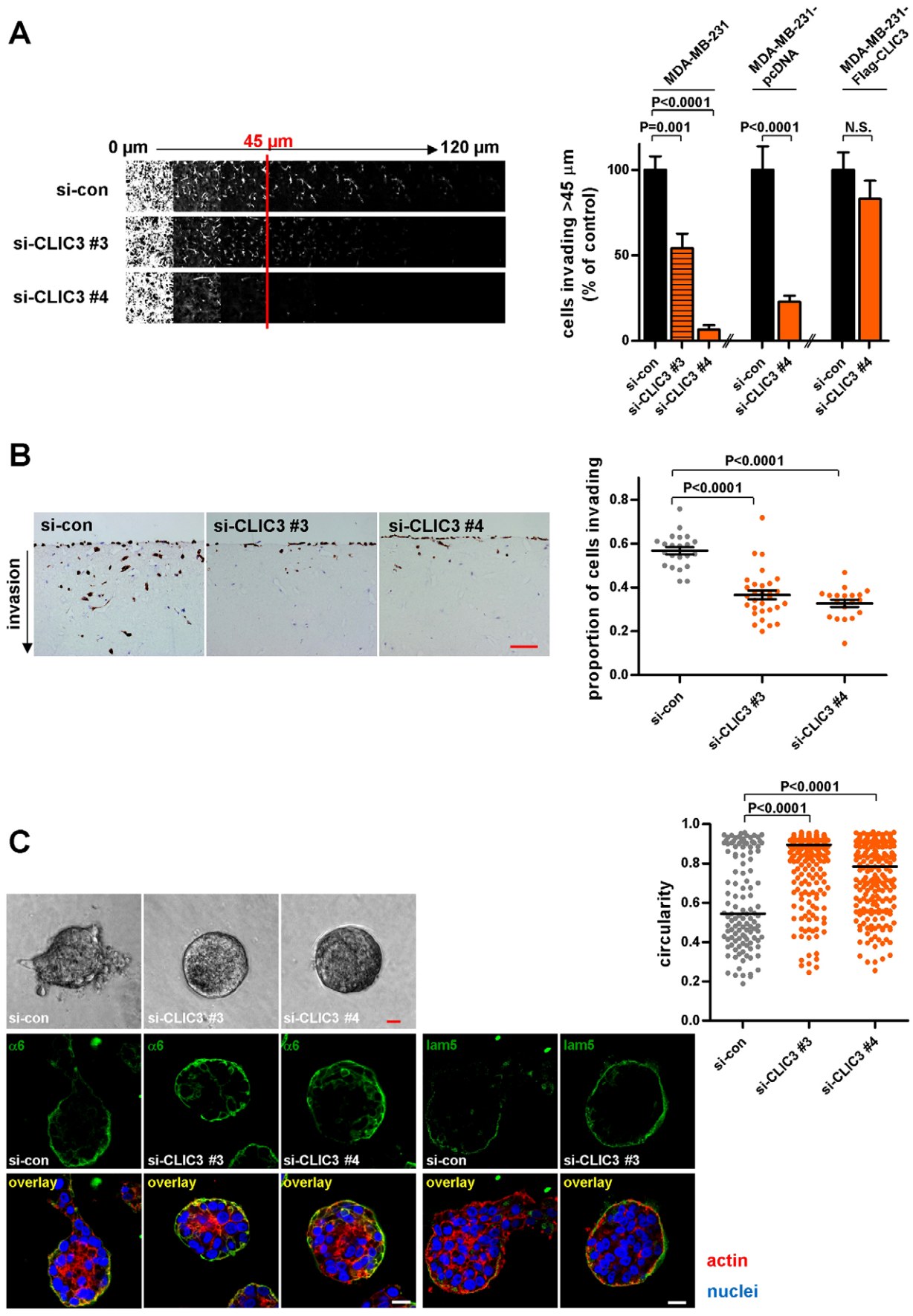

Fig. 2. See next page for legend.

Fig. 2. CLIC3 promotes invasion. (A) MDA-MB-231 cells were nucleofected with non-targeting siRNA (si-con) or siRNAs targeting CLIC3 (si-CLIC3 #3 or #4), then allowed to invade into plugs of fibronectin-supplemented Matrigel. Invasion is quantified as the proportion of cells migrating further than 45 μm. The experiment was repeated using pools of MDA-MB-231 cells with stable expression of empty vector (MDA-MB-231-pcDNA3) or Flag-tagged siRNA-resistant CLIC3 (MDA-MB-231-Flag-CLIC3). Data are mean±s.e.m. from three independent experiments, performed in duplicate; *P*-values were calculated with a Mann–Whitney U test. (B) MDA-MB-231 cells were plated onto a collagen plug that had been pre-conditioned by primary human fibroblasts, allowed to invade for 6 days, then stained for cytokeratin. Scale bar: 100 μm. At least four individual plugs per siRNA duplex were generated in two independent experiments. Values are mean±s.e.m. Each data point represents an individual x10 magnification field. *P*-values were calculated with a Mann–Whitney U test. (C) MCF10DCIS.com cells were plated on a thin layer of Matrigel and phase-contrast micrographs captured after 6 days (upper panels). Individual acini were outlined and circularity determined using ImageJ with a value of 1 representing perfect circularity. Each data point represents a single acinus with data generated in three independent experiments (si-con, $n=121$; si-CLIC3 #3, $n=242$; si-CLIC3 #4, $n=218$); the bar represents the median. *P*-values were calculated with a Mann–Whitney U test. To visualize the basement membrane acini were stained for α6 integrin or laminin 5 (middle panels). The actin cytoskeleton and nuclei were visualized with phalloidin–Alexa-Fluor-546 and DAPI staining respectively (lower panels). Scale bars: 20 μm.

CLIC3 is involved in matrix degradation and invasion but not proliferation

To investigate how CLIC3 might contribute to aggressiveness in breast cancer, we silenced its expression in MDA-MB-231 cells, observing no alteration of growth *in vitro* (supplementary material Fig. S2A,B). We hypothesized that CLIC3 might promote an invasive phenotype similar to that observed in Rab25-expressing ovarian tumors (Dozynkiewicz et al., 2012). However, although Rab25 has been identified as the driver of the 1q22 amplicon, which promotes ovarian cancer aggressiveness (Cheng et al., 2004), it appears to inhibit progression in several other tumor types (Amornphimoltham et al., 2013; Nam et al., 2010; Tong et al., 2012). In ER-negative breast cancer, loss of Rab25 is common (Cheng et al., 2006). MDA-MB-231 cells do not express Rab25 and forced re-expression reduces their invasiveness (Cheng et al., 2010). Consistent with these latter observations, we could not detect any association between Rab25 expression and poor outcome in ER-negative breast cancer, nor any clear indications of collaboration between Rab25 and CLIC3 (supplementary material Fig. S1F). This led us to postulate the presence of a distinct CLIC3-dependent but Rab25-independent pro-invasive pathway in the context of some ER-negative breast carcinomas. Consistent with this hypothesis, two CLIC3 small interfering RNAs (siRNAs) reduced invasion through fibronectin-supplemented Matrigel (Fig. 2A), with invasion rescued by expression of siRNA-resistant CLIC3 (supplementary material Fig. S2C). Silencing CLIC3 expression also reduced invasion into organotypic collagen plugs that had been preconditioned with dermal fibroblasts (Fig. 2B).

A key event in progression from DCIS to invasive carcinoma is proteolytic disruption of the basement membrane. To model this event in 3D culture, we employed ER-negative MCF10DCIS.com mammary cells, which are derived from the 'normal' MCF10A cell line and form well-defined comedo-like DCIS structures when injected as xenografts. However, with time, these lesions spontaneously progress to invasive carcinoma characterized by disruption of their surrounding basement membrane and the development of invasive outgrowths (Behbod et al., 2009; Hu et al., 2008; Miller et al., 2000). Elements of this progression are recapitulated in 3D culture (Jedeszko et al., 2009; So et al., 2013). Indeed, when cultured in Matrigel for 2–4 days, MCF10DCIS.com cells formed non-invasive comedo structures bounded by a basement membrane [as determined by immunofluorescence staining for laminin-5, α6 and β4 integrin and collagen (data not shown)]. However, quantitative morphological analysis indicated that, following 6 days of culture, these comedo-like structures began to lose their sphericity (Fig. 2C), and that this was associated with the appearance of substantial breaches of the basement membrane through which cells invaded into the surrounding Matrigel (Fig. 2C). Silencing of CLIC3 significantly opposed this spontaneous disruption of the basement membrane and loss of acinar sphericity (Fig. 2C; supplementary material Fig. S2D). Taken together, these data implicate CLIC3 in disruption of the basement membrane and the invasive behavior that accompanies DCIS to invasive carcinoma transition.

CLIC3 localizes to a late endosomal/lysosomal compartment

Most CLIC3 in MDA-MB-231 cells was present in vesicles vesicles (Fig. 3A,B). To determine which compartment(s) this represented, we coexpressed mCherry–CLIC3 with markers of early and recycling endosomes (EEA1, Rab4 and Rab11a), late endosomes/lysosomes (Rab7, LAMP1 and Lysotracker Green) and the Golgi (pAcGFP1-Golgi). The majority of CLIC3 was present in vesicles that contained Rab7, LAMP1 or Lysotracker (Fig. 3A; supplementary material Fig. S3A). Thus, in MDA-MB-231 cells, CLIC3 is predominantly localized to the late endosomal/lysosomal system, consistent with previous studies in A2780 ovarian carcinoma cells (Dozynkiewicz et al., 2012).

CLIC3 is required for recycling of internalized MT1-MMP

The involvement of CLIC3, a late endosomal protein, in disruption of the basement membrane – an event that is known to require proteolysis of basement membrane components – led us to consider whether MT1-MMP, a transmembrane matrix metalloproteinase that traffics through late endosomes, was involved (Poincloux et al., 2009). Indeed, siRNA against MT1-MMP reduced invasion of MDA-MB-231 into Matrigel (supplementary material Fig. S4A). Furthermore, the MT1-MMP inhibitor, GM6001, reduced spontaneous loss of comedo sphericity (supplementary material Fig. S4B) and MCF10DCIS.com basement membrane disruption (supplementary material Fig. S4C), indicating involvement of MT1-MMP in these processes. MT1-MMP undergoes endo-exocytic cycling, and previous studies have implicated recycling pathways involving late as well as early endosomes and the trans-Golgi network in returning internalized MT1-MMP to the plasma membrane (Bravo-Cordero et al., 2007; Remacle et al., 2003; Remacle et al., 2005; Wang et al., 2004; Williams and Coppolino, 2011). In MDA-MB-231 cells, MT1-MMP is predominantly localized to late endosomes/lysosomes from where it is recycled to the plasma membrane (Monteiro et al., 2013; Steffen et al., 2008; Yu et al., 2012). Indeed, we found that 21%±1.27 (mean±s.e.m., $n=26$ cells) of endogenous MT1-MMP resided in vesicles that were positive for endogenous CLIC3 (Fig. 3B), and live-cell imaging of mCherry–CLIC3 and GFP–MT1-MMP revealed a subset of vesicles in which these proteins were colocalized and moved together for extended periods (Fig. 3C; supplementary material Fig. S3B; Movie 1).

Journal of Cell Science (2014) 127, 3893–3901 doi:10.1242/jcs.135947

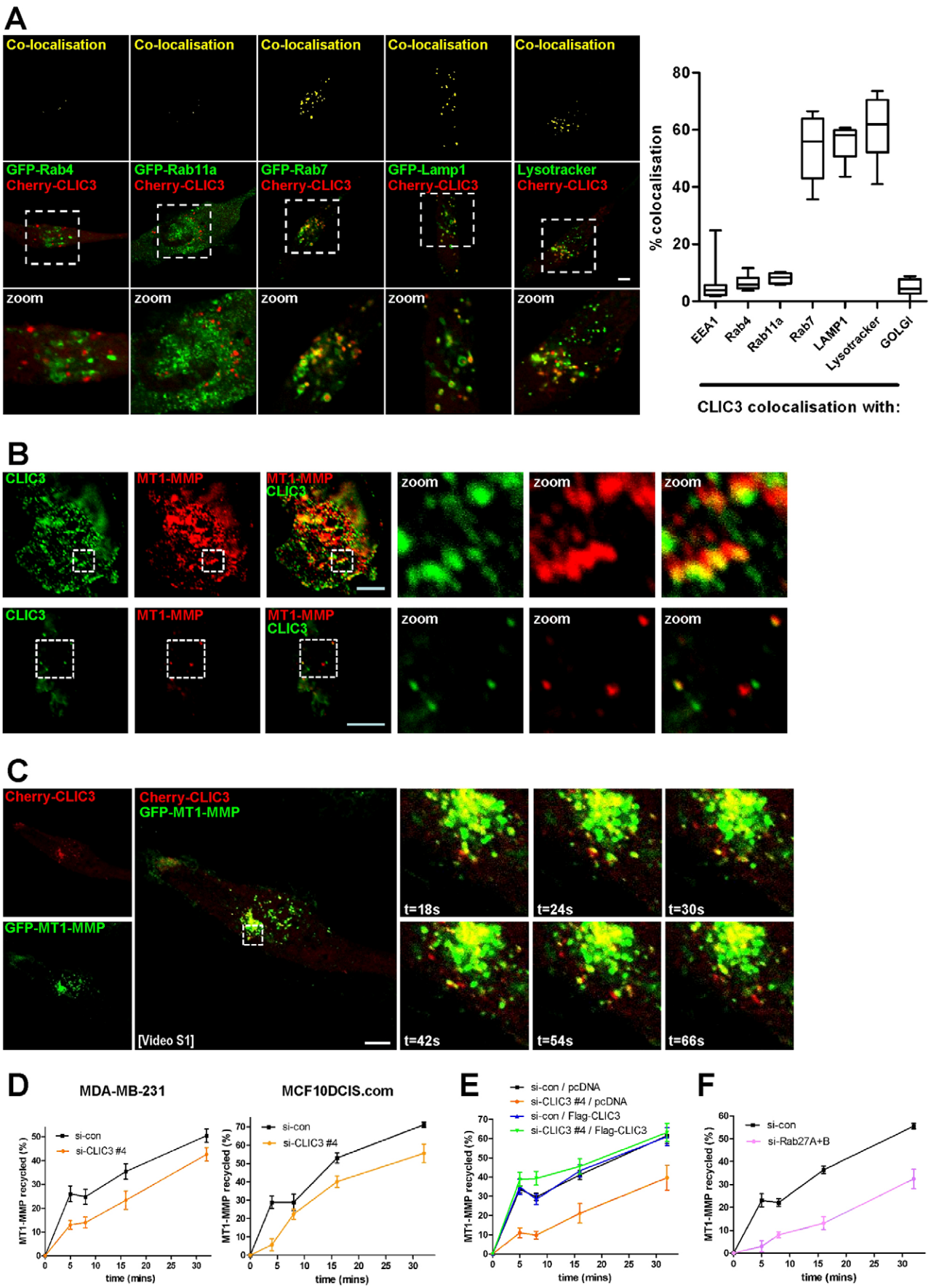

Fig. 3. See next page for legend.

Fig. 3. CLIC3 is localized to the late endosome/lysosome and regulates MT1-MMP recycling. (A) MDA-MB-231 cells expressing fluorescently tagged proteins or exposed to Lysotracker Green were imaged by live-cell confocal microscopy. The zoom panels show a magnified view of the area outline by the dashed square. Right, colocalization is expressed as a percentage of yellow versus red pixels for ≥30 cells from three or more experiments. Box, median and interquartile range; whiskers, minimum to maximum. Scale bar: 10 μm. Single-channel images are presented in supplementary material Fig. S3A. (B) Colocalization of endogenous CLIC3 and MT1-MMP in fixed paraffin-embedded MDA-MB-231 cells. Examples of two separate cells, with differing focal planes are shown in the upper and lower panels respectively. Scale bars: 5 μm. (C) MDA-MB-231 cells expressing GFP–MT1-MMP and Cherry–CLIC3 were imaged by live-cell confocal microscopy. Movies were acquired and stills are shown from the time points indicated. Scale bar: 10 μm. Single-channel images are presented in supplementary material Fig. S3B. (D) MDA-MB-231 or MCF10DCIS.com cells were nucleofected with non-targeting siRNA (si-con) or siRNA targeting CLIC3 (si-CLIC3 #4). Recycling of MT1-MMP was determined as described in Roberts et al. (Roberts et al., 2001). Values are mean±s.e.m. from three independent experiments. (E) MT1-MMP recycling was determined following CLIC3 siRNA nucleofection in MDA-MB-231 cells with stable expression of empty vector (pcDNA3) or Flag-tagged siRNA-resistant CLIC3 (Flag-CLIC3). (F) MDA-MB-231 cells were nucleofected with non-targeting siRNA or siRNAs targeting Rab27A and Rab27B (si-Rab27A+B) and recycling of MT1-MMP determined.

We speculated that CLIC3 might have a role in delivery of internalized functional MT1-MMP from late endosomes back to the plasma membrane. In control MDA-MB-231 and MCF10DCIS.com cells, recycling of MT1-MMP proceeded with bi-phasic kinetics; there was an initial phase of recycling that occurred within 5 min, followed by a period of slower recycling (Fig. 3D). Although the total levels of MT1-MMP were not altered by CLIC3 knockdown (data not shown), the rate at which internalized MT1-MMP was returned to the plasma membrane was reduced, particularly in the initial rapid phase of recycling (Fig. 3D). A more modest effect was observed for α5β1 integrin (data not shown). Recycling of MT1-MMP was rescued by expression of siRNA-resistant CLIC3 (Fig. 3E). It is important to note that the rapid kinetics observed do not necessarily entail 'short loop' Rab4-dependent recycling of MT1-MMP from the early endosome. Indeed, we observed that silencing of Rab27A and Rab27B (supplementary material Fig. S2E), which are established regulators of exocytic trafficking from late endosomal (Ostrowski et al., 2010) and secretory lysosomal compartments (Ménasché et al., 2000), as well as related organelles such as melanosomes (Bahadoran et al., 2001), was sufficient to inhibit rapid recycling of MT1-MMP in a manner similar to that observed with CLIC3 silencing (Fig. 3F).

CLIC3 is required for delivery of MT1-MMP vesicles to the substratum

z-sections taken through the cell body indicated that the amount of vesicular (endogenous and mCherry-tagged) MT1-MMP near the ventral surface of the cell was reduced by CLIC3 knockdown (Fig. 4A,B; supplementary material Fig. S3C). We used total internal reflection fluorescence (TIRF) video microscopy to quantify the appearance of MT1-MMP-containing vesicles very close (<200 nm) to the ventral plasma membrane. Silencing of CLIC3 reduced the number and size of MT1-MMP-containing vesicles that appeared in the TIRF field (Fig. 4C; supplementary Movies 2 and 3), and correspondingly increased the amount of MT1-MMP retained within perinuclear vesicles above the plane of adhesion (Fig. 4B). Expression of siRNA-resistant CLIC3 rescued delivery of MT1-MMP to the TIRF field (Fig. 4D). CLIC3 knockdown did not reduce the amount of LAMP1 vesicles in the TIRF field, indicating that CLIC3 was not required for delivery of late endosomes and/or their docking with the plasma membrane (Fig. 4E; supplementary material Movies 4 and 5). These observations suggest that CLIC3 might act in the perinuclear region to promote the sorting of MT1-MMP into late endosomes destined for the plasma membrane, rather than being necessary to achieve delivery of late endosomes in general.

Collectively, our data identify CLIC3 as a regulator of the sorting and targeting of MT1-MMP containing late endosomes to the ventral plasma membrane, and indicate that CLIC3-dependent delivery of MT1-MMP promotes MT1-MMP-dependent invasiveness. Our previous work identified a collaborative role for CLIC3 and Rab25 to drive α5β1 integrin recycling in ovarian and pancreatic cancer. However, the present study conducted in ER-negative breast cancer cells, including MDA-MB-231 cells that do not express Rab25, reports minor reductions in integrin recycling following CLIC3 knockdown, whereas trafficking of MT1-MMP is strongly dependent on CLIC3. It is perhaps not surprising that non-integrin cargoes of the CLIC3-dependent pathway should not be influenced by Rab25 expression. Indeed, Rab25 associates directly with α5β1 integrin, and in the absence of this interaction this integrin cannot efficiently be targeted to late endosomes (Dozynkiewicz et al., 2012). MT1-MMP, however, can clearly reach CLIC3-positive late endosomes without Rab25. Moreover, invading MDA-MB-231 cells traffic MT1-MMP to invadopodia located towards the leading edge of the cell (Packard et al., 2009; Wolf et al., 2007; Yu et al., 2012), whereas CLIC3-dependent pathways transport α5β1 integrin to the cell rear in Rab25-expressing cells. Therefore, we propose that CLIC3 is involved in late endosomal trafficking to drive invasion in a broad range of tumor types, but that the particular pro-invasive cargo (active integrin versus MT1-MMP) and the site to which recycling is targeted (cell rear versus invadopodia) will depend on the cellular context and expression of GTPases, such as Rab25.

MATERIALS AND METHODS

TMA and survival analysis

Generation of the breast tissue microarray (TMA), CLIC3 immunohistochemistry and use of the weighted histoscore method are described previously (Dozynkiewicz et al., 2012; Ohotski et al., 2012). Protein competition and matched normal and tumor tissue studies utilized TMAs T089 and BR804a respectively (US Biomax). Details of antibodies are in supplementary material Table S2. Ethical approval was granted by the Local Research Ethics Committee and clinical investigation was conducted according to the principles expressed in the Declaration of Helsinki (2000).

Cell culture and nucleofection

MDA-MB-231 cells were cultured and transfected as described previously (Yu et al., 2012). MCF10DCIS.com cells were cultured in Advanced DMEM/F12, L-Glutamine and 5% horse serum and nucleofected using the Amaxa kit T/Program T-020. MDA-MB-231 cells expressing the siRNA-resistant pcDNA3-FLAG-CLIC3 (Dozynkiewicz et al., 2012) or pcDNA3 were generated by selection in G418 (800 μg/ml). siRNA sequences were: CLIC3, no. 3, 5′-AGACAGACACGCUGCAGAU-3′ and no. 4, 5′-CGGACGUGCUGAAGGACUU-3′; non-targeting smartPool; MT1-MMP smartpool; Rab27A and Rab27B smartpools (all Dharmacon). Cherry–CLIC3 and pcDNA3-Flag-CLIC3 constructs were as described previously (Dozynkiewicz et al., 2012). mCherry–MT1-MMP was a gift from Philippe Chavrier (Institute Curie, Paris, France). pAcGFP1-Golgi was from Clontech (Palo Alto, CA). GFP–tensin-1 was a gift from Ken Yamada (NIH, Bethesda). GFP–α5-integrin was a gift from Donna Webb (Vanderbilt, Nashville, TN). EGFP–Rab4, EGFP–Rab11a, LAMP1–YFP and Rab7–GFP were as described previously.

For 3D culture, 5×10^3 MCF10DCIS.com cells/well were plated on a thin layer of Matrigel (40 μl per well; or 5 μl for immunofluorescence

Journal of Cell Science (2014) 127, 3893–3901 doi:10.1242/jcs.135947

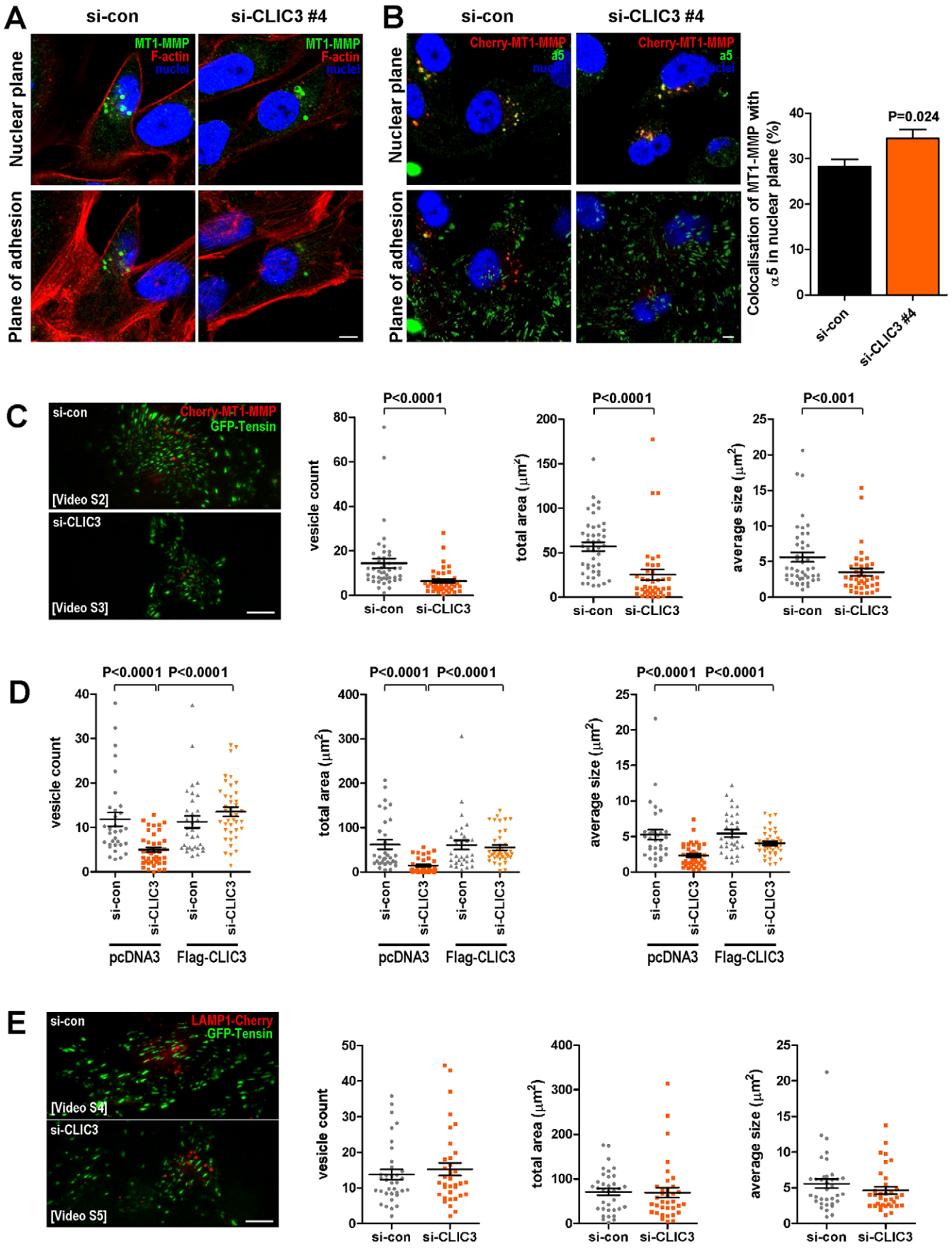

Fig. 4. See next page for legend.

Fig. 4. CLIC3 is required for polarized delivery of CLIC3 vesicles to the substratum. (A) MDA-MB-231 cells were nucleofected with non-targeting siRNA (si-con) or siRNA targeting CLIC3 (si-CLIC3 #4), fixed, and endogenous MT1-MMP detected with an anti-MT1-MMP antibody. Actin was stained with phalloidin–Alexa-Fluor-546 and the nucleus with DAPI. (B) MDA-MB-231 cells were nucleofected with siRNA and Cherry–MT1-MMP, fixed, and endogenous α5 integrin was detected with an anti-α5-integrin antibody and the nucleus with DAPI. Images were captured at both the ventral surface of the cell (plane of adhesion) and at the center of the cell body (nuclear plane) with confocal microscopy. ImageJ was used to quantify the amount of MT1-MMP that colocalized with α5 integrin and is expressed as the percentage of yellow versus red pixels. Values are mean±s.e.m. from three or more experiments ($n \geq 30$ cells). (C) MDA-MB-231 cells were nucleofected with siRNA, Cherry–MT1-MMP and GFP-tagged tensin-1, and imaged with live-cell TIRF microscopy. Quantification of number of MT1-MMP vesicles entering the TIRF field (left), the total area occupied by MT1-MMP vesicles (center) and the average vesicle size (right) are shown with each data point representing an individual cell. (D) MDA-MB-231 cells with stable expression of empty vector (pcDNA3) or Flag-tagged siRNA-resistant CLIC3 (Flag-CLIC3) were nucleofected with siRNA, Cherry–MT1-MMP and GFP-tagged tensin 1, and TIRF microscopy was performed as above. (E) Live-cell TIRF microscopy of MDA-MB-231 cells nucleofected with siRNA, LAMP1–Cherry and GFP-tagged tensin 1. Values are mean±s.e.m. *P*-values were calculated with a Mann–Whitney U test. Scale bars: 10 μm.

studies) in an eight-well chamber slide as previously described (Debnath et al., 2003). Multiple phase-contrast images at ×10 magnification were captured from duplicate wells after 6 days of culture and circularity was determined using ImageJ.

Invasion and recycling assays

Invasion assays were performed as described previously (Hennigan et al., 1994; Timpson et al., 2011). Recycling assays were performed as described previously (Roberts et al., 2001).

Immunofluorescence

Cells were seeded onto glass-bottomed 3-cm plates and imaged with a 64× objective of an inverted confocal microscope (Fluoview FV1000; Olympus), under 5% CO_2 and at 37℃, at 48 h after nucleofection of expression vectors or 30 min after addition of Lysotracker Green DND-26 (Molecular Probes). To image endogenous CLIC3, cells were trypsinized, fixed overnight in 10% neutral buffered formalin, resuspended in 2% agarose and embedded in wax. Proteins were then visualized by immunofluorescence of paraffin sections. To quantify colocalization, the confocal images underwent two rounds of local contrast enhancement (image blurring, subtraction of the blurred image and subsequent contrast enhancement) and threshold adjustment using ImageJ software. The number of yellow pixels was then expressed as a percentage of pixels in the red channel, as previously described (Dozynkiewicz et al., 2012).

Acknowledgements

The breast cancer TMA was constructed by Claire Orange (Pathology Unit, University of Glasgow) and immunohistochemistry performed by Colin Nixon (Histology Service, Beatson Institute for Cancer Research).

Competing interests

The authors declare no competing interests.

Author contributions

I.M. and J.C.N. designed the experiments and wrote the manuscript. I.M., E.R. and L.M. prepared the figures. I.M. and E.R. carried out the majority of the experiments with additional help from J.C.N, L.M., P.V.B., C.S., S.C. and M.D. P.T. carried out the organotypic invasion assay and G.K. analysed gene expression data. J.E. provided the breast TMA.

Funding

This work is supported by Cancer Research UK; and the Breast Cancer Campaign. E.R. is funded by the West of Scotland Women's Bowling Association.

Supplementary material

Supplementary material available online at
http://jcs.biologists.org/lookup/suppl/doi:10.1242/jcs.135947/-/DC1

References

Amornphimoltham, P., Rechache, K., Thompson, J., Masedunskas, A., Leelahavanichkul, K., Patel, V., Molinolo, A., Gutkind, J. S. and Weigert, R. (2013). Rab25 regulates invasion and metastasis in head and neck cancer. *Clin. Cancer Res.* **19**, 1375-1388.

Bahadoran, P., Aberdam, E., Mantoux, F., Buscà, R., Bille, K., Yalman, N., de Saint-Basile, G., Casaroli-Marano, R., Ortonne, J. P. and Ballotti, R. (2001). Rab27a: A key to melanosome transport in human melanocytes. *J. Cell Biol.* **152**, 843-850.

Behbod, F., Kittrell, F. S., LaMarca, H., Edwards, D., Kerbawy, S., Heestand, J. C., Young, E., Mukhopadhyay, P., Yeh, H. W., Allred, D. C. et al. (2009). An intraductal human-in-mouse transplantation model mimics the subtypes of ductal carcinoma in situ. *Breast Cancer Res.* **11**, R66.

Bravo-Cordero, J. J., Marrero-Diaz, R., Megías, D., Genís, L., García-Grande, A., García, M. A., Arroyo, A. G. and Montoya, M. C. (2007). MT1-MMP proinvasive activity is regulated by a novel Rab8-dependent exocytic pathway. *EMBO J.* **26**, 1499-1510.

Cheng, K. W., Lahad, J. P., Kuo, W. L., Lapuk, A., Yamada, K., Auersperg, N., Liu, J., Smith-McCune, K., Lu, K. H., Fishman, D. et al. (2004). The RAB25 small GTPase determines aggressiveness of ovarian and breast cancers. *Nat. Med.* **10**, 1251-1256.

Cheng, J. M., Ding, M., Aribi, A., Shah, P. and Rao, K. (2006). Loss of RAB25 expression in breast cancer. *Int. J. Cancer* **118**, 2957-2964.

Cheng, J. M., Volk, L., Janaki, D. K., Vyakaranam, S., Ran, S. and Rao, K. A. (2010). Tumor suppressor function of Rab25 in triple-negative breast cancer. *Int. J. Cancer* **126**, 2799-2812.

Debnath, J., Muthuswamy, S. K. and Brugge, J. S. (2003). Morphogenesis and oncogenesis of MCF-10A mammary epithelial acini grown in three-dimensional basement membrane cultures. *Methods* **30**, 256-268.

Desmedt, C., Piette, F., Loi, S., Wang, Y., Lallemand, F., Haibe-Kains, B., Viale, G., Delorenzi, M., Zhang, Y., d'Assignies, M. S. et al.; TRANSBIG Consortium (2007). Strong time dependence of the 76-gene prognostic signature for node-negative breast cancer patients in the TRANSBIG multicenter independent validation series. *Clin. Cancer Res.* **13**, 3207-3214.

Dozynkiewicz, M. A., Jamieson, N. B., Macpherson, I., Grindlay, J., van den Berghe, P. V., von Thun, A., Morton, J. P., Gourley, C., Timpson, P., Nixon, C. et al. (2012). Rab25 and CLIC3 collaborate to promote integrin recycling from late endosomes/lysosomes and drive cancer progression. *Dev. Cell* **22**, 131-145.

Frittoli, E., Palamidessi, A., Disanza, A. and Scita, G. (2011). Secretory and endo/exocytic trafficking in invadopodia formation: the MT1-MMP paradigm. *Eur. J. Cell Biol.* **90**, 108-114.

Glück, S., Ross, J. S., Royce, M., McKenna, E. F., Jr, Perou, C. M., Avisar, E. and Wu, L. (2012). TP53 genomics predict higher clinical and pathologic tumor response in operable early-stage breast cancer treated with docetaxel-capecitabine ± trastuzumab. *Breast Cancer Res. Treat.* **132**, 781-791.

Hennigan, R. F., Hawker, K. L. and Ozanne, B. W. (1994). Fos-transformation activates genes associated with invasion. *Oncogene* **9**, 3591-3600.

Hotary, K., Li, X.-Y., Allen, E., Stevens, S. L. and Weiss, S. J. (2006). A cancer cell metalloprotease triad regulates the basement membrane transmigration program. *Genes Dev.* **20**, 2673-2686.

Hu, M., Yao, J., Carroll, D. K., Weremowicz, S., Chen, H., Carrasco, D., Richardson, A., Violette, S., Nikolskaya, T., Nikolsky, Y. et al. (2008). Regulation of in situ to invasive breast carcinoma transition. *Cancer Cell* **13**, 394-406.

Jedeszko, C., Victor, B. C., Podgorski, I. and Sloane, B. F. (2009). Fibroblast hepatocyte growth factor promotes invasion of human mammary ductal carcinoma in situ. *Cancer Res.* **69**, 9148-9155.

Li, X. Y., Ota, I., Yana, I., Sabeh, F. and Weiss, S. J. (2008). Molecular dissection of the structural machinery underlying the tissue-invasive activity of membrane type-1 matrix metalloproteinase. *Mol. Biol. Cell* **19**, 3221-3233.

McGowan, P. M. and Duffy, M. J. (2008). Matrix metalloproteinase expression and outcome in patients with breast cancer: analysis of a published database. *Ann. Oncol.* **19**, 1566-1572.

Ménasché, G., Pastural, E., Feldmann, J., Certain, S., Ersoy, F., Dupuis, S., Wulffraat, N., Bianchi, D., Fischer, A., Le Deist, F. et al. (2000). Mutations in RAB27A cause Griscelli syndrome associated with haemophagocytic syndrome. *Nat. Genet.* **25**, 173-176.

Miller, F. R., Santner, S. J., Tait, L. and Dawson, P. J. (2000). MCF10DCIS.com xenograft model of human comedo ductal carcinoma in situ. *J. Natl. Cancer Inst.* **92**, 1185-1186.

Monteiro, P., Rossé, C., Castro-Castro, A., Irondelle, M., Lagoutte, E., Paul-Gilloteaux, P., Desnos, C., Formstecher, E., Darchen, F., Perrais, D. et al. (2013). Endosomal WASH and exocyst complexes control exocytosis of MT1-MMP at invadopodia. *J. Cell Biol.* **203**, 1063-1079.

Nam, K. T., Lee, H. J., Smith, J. J., Lapierre, L. A., Kamath, V. P., Chen, X., Aronow, B. J., Yeatman, T. J., Bhartur, S. G., Calhoun, B. C. et al. (2010). Loss of Rab25 promotes the development of intestinal neoplasia in mice and is associated with human colorectal adenocarcinomas. *J. Clin. Invest.* **120**, 840-849.

Journal of Cell Science

Ohotski, J., Long, J. S., Orange, C., Elsberger, B., Mallon, E., Doughty, J., Pyne, S., Pyne, N. J. and Edwards, J. (2012). Expression of sphingosine 1-phosphate receptor 4 and sphingosine kinase 1 is associated with outcome in oestrogen receptor-negative breast cancer. *Br. J. Cancer* **106**, 1453-1459.

Ostrowski, M., Carmo, N. B., Krumeich, S., Fanget, I., Raposo, G., Savina, A., Moita, C. F., Schauer, K., Hume, A. N., Freitas, R. P. et al. (2010). Rab27a and Rab27b control different steps of the exosome secretion pathway. *Nat. Cell Biol.* **12**, 19-30; **Suppl.** 1-13.

Packard, B. Z., Artym, V. V., Komoriya, A. and Yamada, K. M. (2009). Direct visualization of protease activity on cells migrating in three-dimensions. *Matrix Biol.* **28**, 3-10.

Perentes, J. Y., Kirkpatrick, N. D., Nagano, S., Smith, E. Y., Shaver, C. M., Sgroi, D., Garkavtsev, I., Munn, L. L., Jain, R. K. and Boucher, Y. (2011). Cancer cell-associated MT1-MMP promotes blood vessel invasion and distant metastasis in triple-negative mammary tumors. *Cancer Res.* **71**, 4527-4538.

Poincloux, R., Lizárraga, F. and Chavrier, P. (2009). Matrix invasion by tumour cells: a focus on MT1-MMP trafficking to invadopodia. *J. Cell Sci.* **122**, 3015-3024.

Remacle, A., Murphy, G. and Roghi, C. (2003). Membrane type I-matrix metalloproteinase (MT1-MMP) is internalised by two different pathways and is recycled to the cell surface. *J. Cell Sci.* **116**, 3905-3916.

Remacle, A. G., Rozanov, D. V., Baciu, P. C., Chekanov, A. V., Golubkov, V. S. and Strongin, A. Y. (2005). The transmembrane domain is essential for the microtubular trafficking of membrane type-1 matrix metalloproteinase (MT1-MMP). *J. Cell Sci.* **118**, 4975-4984.

Rhodes, D. R., Yu, J., Shanker, K., Deshpande, N., Varambally, R., Ghosh, D., Barrette, T., Pandey, A. and Chinnaiyan, A. M. (2004). ONCOMINE: a cancer microarray database and integrated data-mining platform. *Neoplasia* **6**, 1-6.

Roberts, M., Barry, S., Woods, A., van der Sluijs, P. and Norman, J. (2001). PDGF-regulated rab4-dependent recycling of alphavbeta3 integrin from early endosomes is necessary for cell adhesion and spreading. *Curr. Biol.* **11**, 1392-1402.

Sabeh, F., Ota, I., Holmbeck, K., Birkedal-Hansen, H., Soloway, P., Balbin, M., Lopez-Otin, C., Shapiro, S., Inada, M., Krane, S. et al. (2004). Tumor cell traffic through the extracellular matrix is controlled by the membrane-anchored collagenase MT1-MMP. *J. Cell Biol.* **167**, 769-781.

So, J. Y., Smolarek, A. K., Salerno, D. M., Maehr, H., Uskokovic, M., Liu, F. and Suh, N. (2013). Targeting CD44-STAT3 signaling by Gemini vitamin D analog leads to inhibition of invasion in basal-like breast cancer. *PLoS ONE* **8**, e54020.

Steffen, A., Le Dez, G., Poincloux, R., Recchi, C., Nassoy, P., Rottner, K., Galli, T. and Chavrier, P. (2008). MT1-MMP-dependent invasion is regulated by TI-VAMP/VAMP7. *Curr. Biol.* **18**, 926-931.

Szabova, L., Chrysovergis, K., Yamada, S. S. and Holmbeck, K. (2008). MT1-MMP is required for efficient tumor dissemination in experimental metastatic disease. *Oncogene* **27**, 3274-3281.

Têtu, B., Brisson, J., Wang, C. S., Lapointe, H., Beaudry, G., Blanchette, C. and Trudel, D. (2006). The influence of MMP-14, TIMP-2 and MMP-2 expression on breast cancer prognosis. *Breast Cancer Res.* **8**, R28.

Timpson, P., McGhee, E. J., Erami, Z., Nobis, M., Quinn, J. A., Edward, M. and Anderson, K. I. (2011). Organotypic collagen I assay: a malleable platform to assess cell behaviour in a 3-dimensional context. *J. Vis. Exp.* **56**, e3089.

Tong, M., Chan, K. W., Bao, J. Y., Wong, K. Y., Chen, J. N., Kwan, P. S., Tang, K. H., Fu, L., Qin, Y. R., Lok, S. et al. (2012). Rab25 is a tumor suppressor gene with antiangiogenic and anti-invasive activities in esophageal squamous cell carcinoma. *Cancer Res.* **72**, 6024-6035.

Uekita, T., Itoh, Y., Yana, I., Ohno, H. and Seiki, M. (2001). Cytoplasmic tail-dependent internalization of membrane-type 1 matrix metalloproteinase is important for its invasion-promoting activity. *J. Cell Biol.* **155**, 1345-1356.

Ueno, H., Nakamura, H., Inoue, M., Imai, K., Noguchi, M., Sato, H., Seiki, M. and Okada, Y. (1997). Expression and tissue localization of membrane-types 1, 2, and 3 matrix metalloproteinases in human invasive breast carcinomas. *Cancer Res.* **57**, 2055-2060.

Wang, X., Ma, D., Keski-Oja, J. and Pei, D. (2004). Co-recycling of MT1-MMP and MT3-MMP through the trans-Golgi network. Identification of DKV582 as a recycling signal. *J. Biol. Chem.* **279**, 9331-9336.

Williams, K. C. and Coppolino, M. G. (2011). Phosphorylation of membrane type 1-matrix metalloproteinase (MT1-MMP) and its vesicle-associated membrane protein 7 (VAMP7)-dependent trafficking facilitate cell invasion and migration. *J. Biol. Chem.* **286**, 43405-43416.

Wolf, K., Wu, Y. I., Liu, Y., Geiger, J., Tam, E., Overall, C., Stack, M. S. and Friedl, P. (2007). Multi-step pericellular proteolysis controls the transition from individual to collective cancer cell invasion. *Nat. Cell Biol.* **9**, 893-904.

Yu, X., Zech, T., McDonald, L., Gonzalez, E. G., Li, A., Macpherson, I., Schwarz, J. P., Spence, H., Futó, K., Timpson, P. et al. (2012). N-WASP coordinates the delivery and F-actin-mediated capture of MT1-MMP at invasive pseudopods. *J. Cell Biol.* **199**, 527-544.